

Order–Disorder Transition Temperature Depression of a Diblock Copolymer Induced by the Addition of a Random Copolymer

Dae-Cheol Kim, Hwan-Koo Lee, Byeong-Hyeok Sohn, and Wang-Cheol Zin*

Department of Materials Science & Engineering and Polymer Research Institute,
Pohang University of Science & Technology, Pohang 790-784, Kyungbuk, Korea

Received April 5, 2001

ABSTRACT: The change in the order–disorder transition temperature (T_{ODT}) of a diblock copolymer, induced by the addition of a random copolymer, was investigated with synchrotron small-angle X-ray scattering and differential scanning calorimetry techniques. The studied block copolymer was poly(styrene-*b*-butadiene) containing 52 wt % styrene, and the added random copolymer was a small amount of poly(styrene-*r*-butadiene) containing 50 wt % styrene. The observed transition from the isotropic melt to the lamellar ordered structure appeared as a pronounced discontinuity in the peak's height and shape, and the estimated T_{ODT} was found to decrease as the fraction of a random copolymer increased within the solubility limit (about 15 wt %). It was noted that the interdomain distance (D) decreased slightly upon the addition of a random copolymer, suggesting that the added random copolymer may have dissolved into the interfacial region of the microdomain. The plot of the reciprocal scattering maximum $S^{-1}(q^*)$ as a function of the reciprocal absolute temperature T^{-1} can be fitted satisfactorily to the theoretical prediction based on the work of Fredrickson and Helfand. Also, the shift of T_{ODT} in the blend is calculated with the theoretical prediction developed by Whitmore and Noolandi. The spinodal temperature (T_s) and the T_{ODT} decreased along a similar slope with the addition of a random copolymer.

Introduction

Diblock copolymers, when cooled from the melt, undergo an order–disorder transition (ODT)^{1,2} at a certain temperature and form spatially periodic microdomain structures induced by microphase separation because the connectivity of each constituent block prevents the usual macroscopic phase separation observed in homopolymer blends. In the weak segregation regime above the T_{ODT} , Leibler¹ has presented a scattering theory for the phase behavior of diblock copolymers in the framework of random phase approximation (RPA).³ Leibler's theory¹ provides an expression for the scattering function of diblock copolymer melts in the disordered phase. Also, the phase diagram is constructed by the relative chain composition f and the product χN of Flory–Huggins interaction parameter χ and the number of statistical length N .

As for blends containing diblock copolymers, many studies have investigated the phase behavior in binary mixtures of diblock copolymer and homopolymer.^{4–10} Nojima and Roe undertook studies on diblock copolymer (A–B)/homopolymer (A) blend.¹⁰ They showed (1) that, when a small amount of A is dissolved into A–B, the spinodal temperature (T_s) is either elevated or lowered according to the molecular weight ratio of A over A–B and (2) that the magnitude in the change of T_s is higher with larger amounts of added homopolymer. Also, there have been some works^{11–16} on block copolymer/block copolymer blends, or block copolymer/random copolymer blends, which are expected to exhibit a different phase behavior from diblock copolymer/homopolymer blends. The miscibility between the constituent polymers and the change in morphology of diblock copolymer induced by the addition of other polymer were examined as a function of molecular weight ratio and the concentration

of each component. In addition to the above works, the extension to diblock copolymer solutions with a neutral (nonselective) solvent has been carried out.^{17–20} One expects that, if the solvent is a good solvent of roughly equal affinity for both of the blocks, the copolymer solution will have thermodynamics similar to that of the pure melt. It has been shown that there is a tendency for a neutral good solvent to accumulate at the interfaces of the microdomains to screen the unfavorable A–B monomer contacts at the interfaces. On the other hand, there has been no experimental work on the ODT behavior of diblock copolymer (A–B) blends containing a small amount of random copolymer (ABR) having a composition similar to that of diblock copolymer.

In the present work, the effect of added random copolymer (ABR) on the diblock copolymer (A–B) was studied by synchrotron small-angle X-ray scattering (SAXS) and differential scanning calorimetry (DSC). The studied diblock copolymer is poly(styrene-*b*-butadiene) containing 52 wt % styrene (S-B52), and the added random copolymer is poly(styrene-*r*-butadiene) containing 50 wt % styrene (SBR50). From a thermodynamic point of view, it is expected that, at temperatures above the T_{ODT} , SBR50 is homogeneously mixed with S-B52 since the composition of SBR50 is similar to that of S-B52. On the other hand, at temperatures below the T_{ODT} where S-B52 has lamellar morphology, SBR50 will have poor solubility to S-B52 due to the endothermic interaction between SBR50 and both blocks of S-B52 ($\chi_{\text{RS}} \approx \chi_{\text{RB}} \approx 0.5\chi_{\text{SB}}$), since SBR50 contains both styrene and butadiene with equal amount as S-B52. Therefore, added SBR50 is thought to dissolve at the interface of the S-B52 microdomains to reduce unfavorable interaction between SBR50 and S-, B- monomers of S-B52.

In this context, we focused our attention on the change of the T_{ODT} of S-B52 induced by the addition of a small amount of SBR50. We then compared our

* To whom correspondence should be addressed. Tel +82-54-279-2136; Fax +82-54-279-2399; E-mail wczin@postech.ac.kr.

Table 1. Characteristics of Copolymers Used in This Study

brief	copolymer	composition (wt %) ^a styrene	unsaturation ^a		mol wt	
			% trans	% vinyl	M_w^b	M_w/M_n^b
S-B52 ^c	poly(styrene- <i>b</i> -butadiene)	52	45	31	26 000	1.04
SBR50 ^c	poly(styrene- <i>r</i> -butadiene)	50	55	27	24 000	<1.10

^a Obtained from ¹H NMR. ^b From GPC. ^c Synthesized specifically by Dr. H. L. Hsieh of Phillips Petroleum Co. These copolymers are the same materials used in refs 24 and 25, respectively.

experimental results with the Brazovskii–Leibler–Fredrickson–Helfand (BLFH) fluctuation corrected theory for scattering from diblock copolymer.^{21–23} From SAXS experiments, the scattering profile and the effect of fluctuations on it near ODT were obtained over the entire temperature range from a disordered state via ODT to an ordered state. The plot of $S^{-1}(q^*)$ against T^{-1} enabled us to find the T_{ODT} , and this plot could be fitted to the theoretical function of BLFH.²¹ The T_S predicted by Leibler was estimated by the linear regression of fitted results from a very high temperature and was compared with experimentally measured T_{ODT} . The change in the interdomain distance of S-B52 on the addition of SBR50 will also be discussed.

Experimental Section

The samples were mixtures of poly(styrene-*b*-butadiene) containing 52 wt % styrene and a small amount of poly(styrene-*r*-butadiene) containing 50 wt % styrene. The blend samples with various ϕ_{SBR50} from 0 to 0.1 were prepared by first dissolving a predetermined amount of each copolymer in toluene in the presence of an antioxidant (Irganox 1010, Ciba-Geigy Group) and then by slow evaporation of the solvent at room temperature. To remove the residual solvent, the samples were further dried under a vacuum at about 60 °C for over a day. After complete removal of the solvent, the samples were further annealed at 120 °C for 24 h. Detailed copolymer information is listed in Table 1.

Synchrotron SAXS measurement was performed at the 4C1 X-ray beamline of the Pohang Accelerator Laboratory (PAL). Scattering patterns were obtained from a diode-array positional sensitive detector with a wavelength of 1.542 or 1.608 Å. A beam path was maintained under a vacuum to reduce air scattering, and tungsten foil (50 μm) was used for primary beam protection. The measured intensity was corrected for background scattering, detector noise, and absorption by the sample. Each sample was heated far above the melt state and then cooled to room temperature at the rate of −5 °C/min while the intensity data were collected through the detector and computer interface every minute for 20 s. Since the reproducibility was shown between the heating and cooling results, we used the cooling data in the present work. Thermal analysis was performed with a differential scanning calorimeter (Perkin-Elmer DSC7) under the same experimental conditions as the SAXS experiments, and T_{ODT} was determined from the change of exothermic enthalpy during the cooling scan. Glass transition temperatures were measured during reheating at a rate of 20 °C/min after the samples had been held at 150 °C and then cooled to −150 °C at −20 °C/min.

Structure Factor

According to Leibler,¹ the reciprocal structure factor for the melt of diblock copolymer A–B in the mean-field approximation is given by

$$S^{-1}(q) = \frac{F(x, f)}{N} - 2\chi \quad (1)$$

where $x = R_G^2 q^2$ and $f = N_A/N$ (describes the block composition). Following the method for obtaining the function $F(x, f)$ by use of de Gennes's random phase approximation,¹ Nojima and Roe evaluated $F(x, f)$ for

blends of a diblock copolymer and other polymers.¹⁰ $F(x, f)$ reaches its minimum at x^* , corresponding to a maximum in the scattering curve at the nonzero scattering vector q^* , and $S^{-1}(q^*)$ diverges at spinodal temperature. Accordingly, we have $F(x^*, f) = 2(\chi N)_S$. The temperature dependence of the Flory–Huggins interaction parameter is described by

$$\chi(T) = a + b/T \quad (2)$$

In theory, the χ parameter is related to monomer–monomer interactions and thus should be independent of molecular weight and composition of the mixture. Since $F(x, f)$ is independent of χ , and thus on temperature, a plot of the reciprocal scattering intensity at the maximum of $S^{-1}(q^*)$ against the reciprocal absolute temperature T^{-1} shows a linear relationship with a slope of $-2b$. The reciprocal spinodal temperature (T_S^{-1}) can be obtained from an extrapolation to $S^{-1}(q^*) = 0$.

However, going beyond the mean-field picture, the second-order transition pointed out by Leibler for symmetric diblock copolymers was suppressed, and the weak first-order transition appeared at lower temperature.^{26,27} In a non-mean-field regime near the T_{ODT} , nonlinear effects of composition fluctuations appear, and a weak stretching of the chain has been observed.²⁸ Such a fluctuation effect, neglected in the mean-field treatment, was found to be significant for the finite molecular weights usually encountered. An earlier study by Brazovskii has demonstrated that thermally induced composition fluctuation suppresses the critical point and produces a weak first-order transition on a particular class of physical systems.²⁹ Leibler pointed out that a symmetric diblock copolymer melt belongs to this class. Hence, symmetric or near-symmetric diblock copolymers, as a consequence of the connectivity of the blocks, are expected to exhibit first-order transition rather than critical behavior. As the ODT approaches, composition fluctuation grows as the respective block mix into the opposite phase, and the junctions between blocks delocalize from the interface region. This fluctuation was explained by Fredrickson and Helfand^{21–23} following a Hartree approximation developed by Brazovskii.²⁹ The incompressible BLFH fluctuation corrected theory for the structure factor of diblock copolymers is as follows:

$$S^{-1}(q) = \frac{F(x, f)}{N} - 2\chi + \frac{c^3 d \lambda}{N^2} S^{1/2}(q^*) \quad (3)$$

where c , d , and λ are constants defined in ref 17. It is noted that in the Hartree approximation²⁹ the scattering curve retains its shape and the position of maximum q^* . Since the last term in eq 3 is independent of q , it is only the peak height that is affected. Approaching the ODT, the intensities are lower than those expected from Leibler's theory. With eq 3 (which includes the concentration fluctuation in the weak segregation regime) the plot of $S^{-1}(q^*)$ as a function of T^{-1} should exhibit a pronounced deviation from the linear relationship ap-

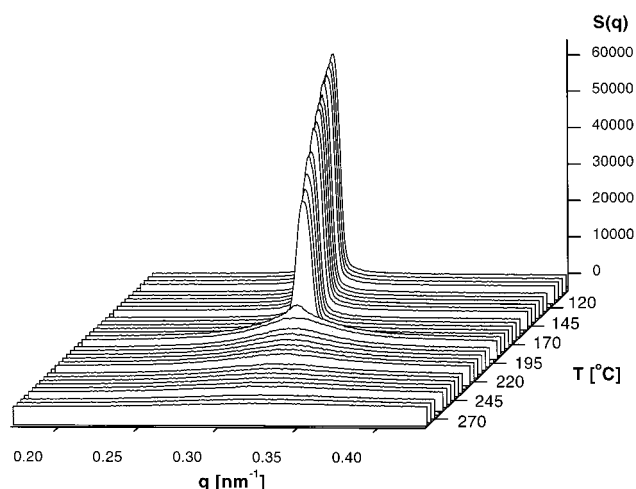


Figure 1. Plot of the measured intensity $S(q)$ of the S-B52 containing 5 wt % of SBR50 as a function of q and T during the cooling cycle from 280 to 50 °C.

proaching the ODT. BLFH theory predicts that the χN value for the symmetric diblock copolymers at the order–disorder transition is $10.495 + 41.022N^{-1/3}$.

Results and Discussion

From the SAXS experiments, the intensity data have been obtained with S-B52/SBR50 having various SBR50 weight fractions from 0 to 0.1. From the plot of $S(q)$ against the scattering vector q ($4\pi\lambda^{-1}\sin\theta$) in the low-temperature region (strong segregation regime), first and third Bragg peaks for the S-B52 having 52 wt % styrene appeared at $q = 0.29$ and 0.88 nm^{-1} , respectively. Thus, the ordered morphology of S-B52 is lamellar as evidenced by the ratios of the peak scattering vectors. The first peak ($D = 2\pi/q^*$) corresponds to a lamellar interdomain spacing of 22.5 nm. On the basis of the discontinuity in the plot of $S^{-1}(q^*)$ vs T^{-1} , the T_{ODT} of S-B52 was found to be 186 °C.

Figure 1 shows the measured structure factor $S(q)$ for the S-B52/SBR50 containing 5 wt % of SBR50, plotted against q during the cooling scan. The ODT from a disordered state to an ordered structure appears as a

pronounced discontinuity in the peak's shape and height. T_{ODT} is 167 °C, at which an abrupt increase of the intensity is clearly seen. Since the ODT is a first-order transition, the process of microdomain formation is similar to the crystallization in common solid systems that shows a highly ordered structure below the T_{ODT} . The narrow peak below T_{ODT} is the first Bragg reflection of the lamellar microdomain periodic structure. The broad peak that persists above T_{ODT} is a Leibler-type peak resulting from density fluctuation originating from the correlation hole effect.³⁰ Repulsive interactions between styrene and butadiene drive local physical clustering of like segments, and this process results in a finite size stabilization of the disordered state on the microdomain length scale.³¹ It is evident that, below the T_{ODT} , the Bragg peak shifts to the smaller q value as the temperature further decreases. This indicates that the interdomain distance increases as T decreases, which is due to the decrease of the conformational entropy of S-B52 chain followed by the increase of its end-to-end distance.

Figure 2 shows the reciprocal scattering maximum $S^{-1}(q^*)$, plotted against the reciprocal absolute temperature T^{-1} for the S-B52/SBR50. Each T_{ODT} was determined from the discontinuity in Figure 2. It is clear that the plots of $S^{-1}(q^*)$ against T^{-1} retain their shape except that they shift to the right side as the fraction of SBR50 increases; thus, it results in T_{ODT} depression. This suggests that, since the scattering from SBR50 is negligible above the ODT, temperature-dependent scattering behavior of S-B52 (the plots of $S^{-1}(q^*)$ against T^{-1}) is not affected on the addition SBR50. Instead, T_{ODT} decrease gradually from an increase of mixing entropy upon mixing between disordered S-B52 and SBR50. Even far above the T_{ODT} , the strong tendency of like blocks to physically cluster results in a fluctuation stabilized disordered phase,²¹ which induces deviation from a linearity in $S^{-1}(q^*)$. Because of a lack of sufficient data above the highest measurement temperature (280 °C), we cannot find a transition from a curved (fluctuation) to a linear (mean-field) form in the data presented in Figure 2. However, the composition fluctuations are clearly evident above the T_{ODT} , and this fluctuation process suppresses the spinodal and critical character-

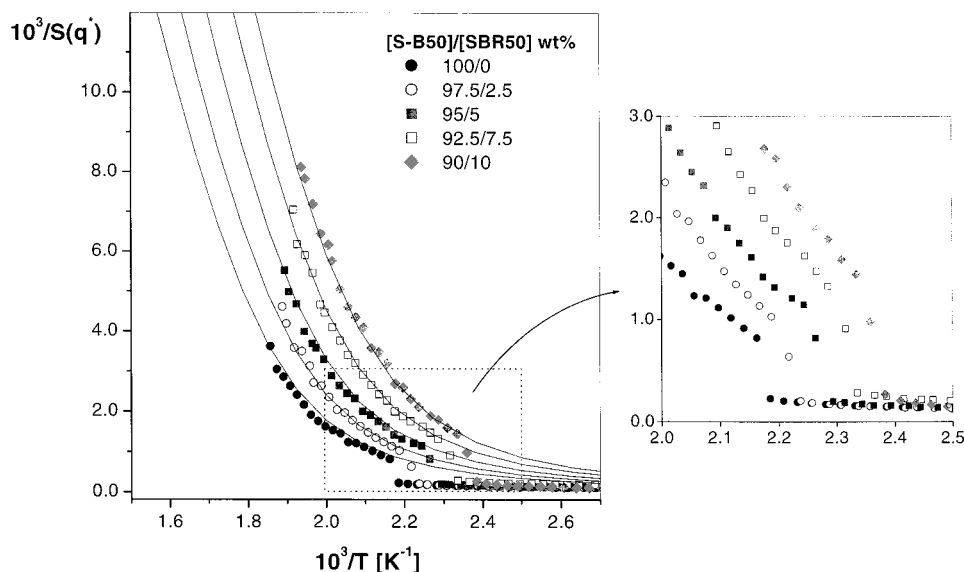


Figure 2. Reciprocal scattering maximum $S^{-1}(q^*)$ is plotted against T^{-1} . T_{ODT} is obtained from the discontinuity of each plot (T_{ODT} for S-B52 is 186 °C).

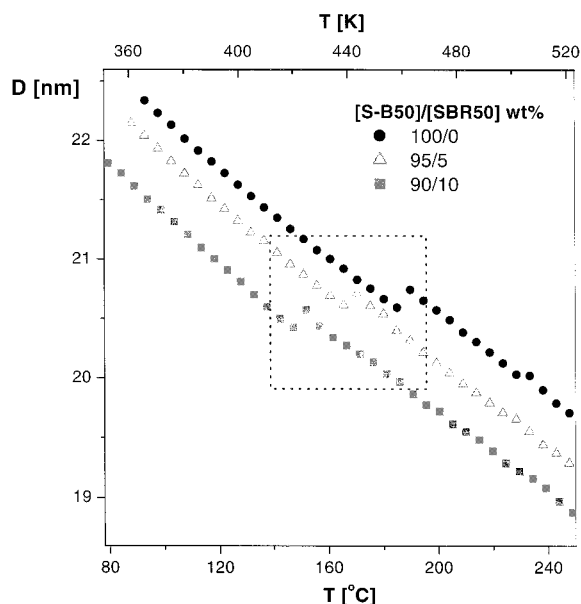


Figure 3. Temperature dependence of interdomain distance (D). D is determined from the scattering vector q^* at the first-order scattering maximum ($D = 2\pi/q^*$).

istics of mean-field theory (second-order transition). The solid lines represent the nonlinear fit of the experimental data to eq 3, and we can see a close resemblance of the experimental result with theoretical predictions. To compare the experimental results to theoretical ones, the experimental intensity data were multiplied with fixed constants for matching the plot scale. For the curve fit, the following common parameters are used: χ (interaction parameter) = $-0.00096 + 18.78/T$ obtained by Ruland et al.,³² N (the number of statistical length) = 347 for S-B52 and 305 for SBR50 (the reference volume is $72.11 \text{ cm}^3/\text{mol}^{32}$). λ is considered a fitting parameter and is obtained empirically from a fitting procedure. The obtained value ($\lambda = 25$) is much smaller than the one predicted by the theory ($\lambda = 105$).²¹ This difference is also shown by the work of Ruland et al.³² The spinodal temperature (T_s) was determined by extrapolating $S^{-1}(q^*)$ from the very high-temperature region to 0 in Figure 2. The χN value at the order-disorder transition, $(\chi N)_{\text{ODT}}$, of a S-B52 determined from the χ parameter above ($T_{\text{ODT}} = 186 \text{ }^\circ\text{C}$ or 459 K) is ~ 13.87 . This value lies within the predictions of Leibler in the limit of infinite molecular weight, $(\chi N)_{\text{ODT}} = 10.50$, and the BLFH theory for $N = 347$, $(\chi N)_{\text{ODT}} = 16.33$.

The change in lamellar interdomain distance (D) with temperature is shown in Figure 3. $D (=2\pi/q^*)$ is determined from the scattering vector q^* at the first-order scattering maximum. In the disordered state, D corresponds to the spatial extent of concentration fluctuations, which are activated by thermal energy, whereas in the ordered state, it corresponds to the spacing for the lamellar microdomain structures generated by the block segregation. As temperature is lowered below the T_{ODT} , the order-disorder transition occurs, and Gaussian chains extend into the ordered state. D increases with a constant slope due to the chain stretching to form a microdomain arising from the attractive interaction between like blocks. (There can be seen an increase of D from 19 to 22 nm [$\sim 30 \text{ \AA}$].) Note in Figure 3 that there is a discontinuous change of D upon lowering the temperature across the T_{ODT} . The change

of D at the T_{ODT} was reported earlier by Stühn,²⁶ Floudas,²⁷ and Hashimoto.³³ Stühn et al.²⁶ reported a discontinuous change of D upon ordering for a SI diblock copolymer forming lamellar microdomains. Discontinuity in D may be expected since ODT is weak first order; D represents two different physical quantities above and below the ODT.

We observe in Figure 3 that D slightly decreases on the addition of SBR50 within the whole temperature range (22.5–22 nm). The decrease of the microdomain spacing of diblock copolymers by the addition of homopolymers was already reported in Winey et al.'s study.⁹ On the blend system of poly(styrene-*b*-isoprene) (PSI)/polystyrene (PS), they found that only the very low molecular weight PS (2.6K) could decrease D of the microdomain structure of the PSI (48.7K). However, the decrement of D as shown in Figure 3 occurs when a SBR50 of similar molecular weight (24K) is added into the S-B52 (26K). This phenomenon can be explained by considering the localization of SBR50 between the junction points at the S-B52 interface. Unlike the homopolymer that is localized into either the S- or B-domain causing the axial microdomain size to increase, SBR50 might be dissolved in the interfacial region of the S-B52 lamellar domain with a simple density distribution centered at the interface since SBR50 has low solubility to both of S- and B- domain of S-B52. That is, the addition of SBR50 induces expansion of the junction points at the interface to increase the lateral microdomain size of S-B52. Thus, added SBR50 induces slight axial contraction in the microdomain structure of S-B52. Although the blends presented in this work are S-B52/SBR50 containing SBR50 between 0 and 10 wt %, it should be noted that macroscopic phase separation may occur above the solubility limit of SBR50 (about 15 wt %).³⁴

Also, the change of D on the addition of SBR50 was compared with the expected change from dilution approximation developed by Whitmore and Noolandi.³⁵ They assumed that when the neutral solvent is added to diblock copolymer, there is no variation in solvent density throughout the microdomain of that diblock copolymer. In dilution approximation, D scales with the concentration of that diblock copolymer:

$$D \approx \varphi_{\text{S-B52}}^\nu \quad \text{or} \quad \ln D \approx \nu \ln \varphi_{\text{S-B52}}$$

The scaling exponent ν is calculated from a linear fit on the plot of D vs $\varphi_{\text{S-B52}}$ for a given temperature. Dilution approximation predicts that ν is 0.22 for strong segregation regimes ($T \ll T_{\text{ODT}}$) and 0.4 near the T_{ODT} . In the plot of $\ln D$ as a function of $\ln \varphi_{\text{S-B52}}$, linearity was clearly observed, and the measured ν was 0.23 at $120 \text{ }^\circ\text{C}$. At $180 \text{ }^\circ\text{C}$, slightly below the T_{ODT} , ν was 0.28, showing a tendency to approach the value 0.4.

The DSC first cooling traces of S-B52/SBR50 is seen in Figure 4. Although the change in heat on ODT is minute ($\Delta H \approx 4 \times 10^{-3} \text{ cal/g}$), we can see an exothermic enthalpy change which indicates a weak first-order transition from a disordered phase to an ordered lamellar microdomain. In accordance with the results from SAXS experiments, T_{ODT} gradually decreases as the fraction of SBR50 increases.

Also, glass transition temperatures were recorded to better understand the morphology after ordering takes place. Figure 5 represents the DSC heating traces of S-B52/SBR50 with different SBR50 contents. As shown

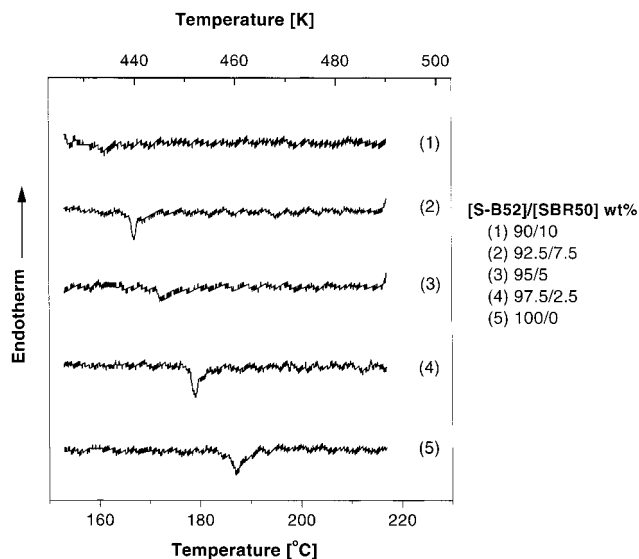


Figure 4. DSC traces ($-5\text{ }^{\circ}\text{C}/\text{min}$) recorded during the first cooling scan. T_{ODT} gradually decreases as the fraction of SBR50 increases.

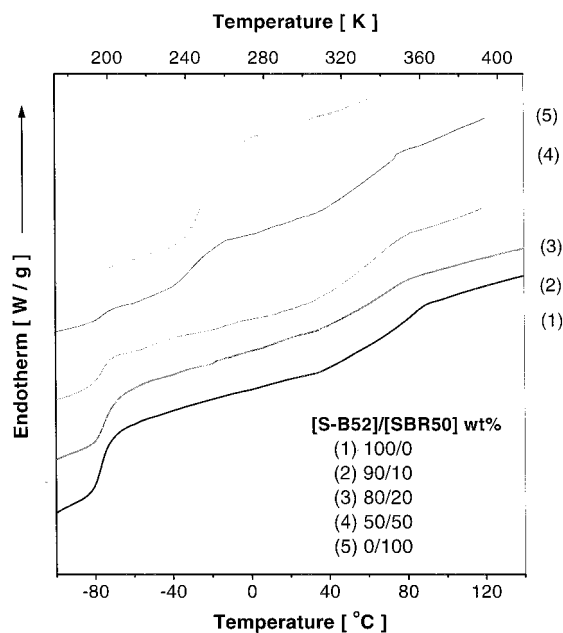


Figure 5. DSC traces ($20\text{ }^{\circ}\text{C}/\text{min}$) of S-B52/SBR50 recorded during the second heating scan. Glass transition temperature was measured from the endothermic heat change.

in Figure 5, S-B52 shows two T_g s of $-77\text{ }^{\circ}\text{C}$ for the PB microdomain and $83\text{ }^{\circ}\text{C}$ for the PS microdomain. The T_g of the amorphous SBR50 is $-24\text{ }^{\circ}\text{C}$. S-B52/SBR50 containing 10 wt % of SBR50 shows only two T_g s similar to those of S-B52, indicating that macroscopic phase separation does not occur. On the other hand, for S-B52/SBR50 containing 50 wt % of SBR50, three T_g s are observed, indicating the existence of the SBR50 domain which is macroscopically phase separated from the S-B52 microdomain. Since the two T_g s of S-B52 do not differ within experimental error as SBR50 content increased, solubilized SBR50 might mainly dissolve into the interface of the S-B52 microdomain rather than in both S- and B-domains. Considering the result from light scattering experiments on S-B52/SBR60, which is a similar system to S-B52/SBR50, S-B52/SBR60 showed a macroscopically phase-separated state when the SBR60 content was larger than about 15 wt %.³⁴

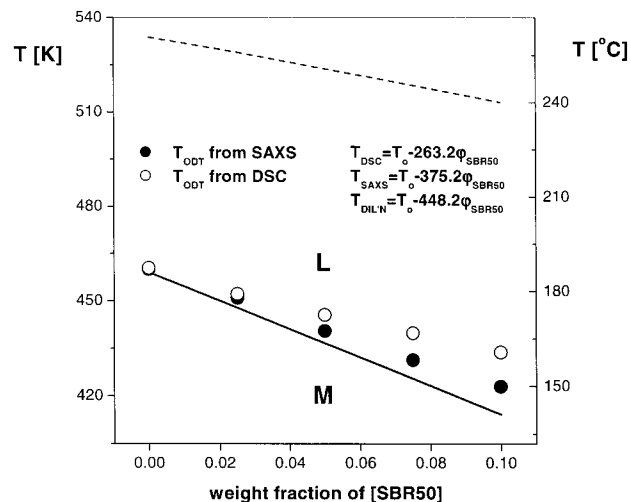


Figure 6. Results from the SAXS and DSC studies on S-B52/SBR50. Solid circles denote the T_{ODT} obtained from SAXS results, and open circles are T_{ODT} estimated from DSC experiments. The solid line calculated is T_{ODT} from dilution approximation; the dashed line represents the T_S .

In Figure 6, order-disorder transition temperatures obtained from the SAXS and DSC experiments are plotted against the weight fraction of SBR50. The "L" phase above the transition line indicates the homogeneous mixed phase of the S-B52 and the SBR50 in the disordered state. The "M" phase below the transition line indicates the ordered microdomain structure of the S-B52 mixed with the SBR50. Both T_{ODT} and T_S decreased as the SBR50 volume fraction increases. Although there was slight difference in the slope of T_{ODT} measured by the SAXS and DSC experiments, T_{ODT} was lowered with a linear slope upon the addition of small amount of SBR50. The T_{ODT} depression with increasing the amount of SBR50 can be understood from the analogy that added SBR50 increases mixing entropy without increasing the enthalpy on mixing into disordered S-B52. We compared the experimental results with dilution approximation for the shift of T_{ODT} . The solid line is the T_{ODT} calculated with dilution approximation.³⁵ The dilution approximation gives an expression for the shift of T_{ODT} as follows:

$$T_{\text{ODT}}/T_0 = 1 - (1 + aT_0/b)\phi_{\text{SBR}}$$

where T_{ODT} and T_0 are the ODT of the blend and S-B52, respectively, and $\chi = a + b/T$.

The T_{ODT} calculated with dilution approximation decreases with a more negative slope than those from experimental results. Although the basic feature is similar, this discrepancy may occur, since SBR50 is not homogeneously mixed as dilution approximation assumes, but might be localized into the interface of the S-B52 microdomain.

The dashed line is the T_S calculated by linear regression of the fitted results in Figure 2 from a very high temperature. This lies at temperatures much higher than T_{ODT} (about 80 K). Although spinodal serves as a classical limit for the expansion and has no longer the physical meaning of stability limit, both T_{ODT} and T_S are the measure of the stability of the phase from a different point of view. Since T_{ODT} and T_S indicate the thermodynamic stability of the phase transition between a disordered phase and an ordered one, they may show an equal response upon the addition of SBR50 to give

the same slope in the S-B52-rich region. Thus, the trends in temperature depression for both T_{ODT} and T_S may be similar.

Conclusions

From the SAXS study, the order–disorder transition was studied on S-B diblock copolymer containing a small amount of SBR random copolymer. The transition was shown to be discontinuous and was accompanied by strong concentration fluctuations in accordance with theoretical expectations. T_{ODT} was found to decrease gradually on the addition of SBR. This phenomenon is similar to the melting point depression occurring in crystal/solvent systems where the solvent is homogeneously mixed in melt with the increase of mixing entropy upon mixing between disordered crystal and solvent. It is noted that, below the T_{ODT} , SBR is not homogeneously mixed but might be localized into the interface of the S-B microdomain, since SBR has low solubility to either S- or B-domain of S-B. Thus, a contraction of the S-B interdomain distance takes place. Above the T_{ODT} , attention has been focused on fluctuation stabilization in the disordered state. The plots of measured $S^{-1}(q^*)$ as a function of T^{-1} were well fitted to the fluctuation theory of BLFH, with suitable parameters chosen. This fluctuation process suppressed the spinodal divergence of mean-field theory, and the T_{ODT} appeared at much lower temperatures in comparison to the classical T_S suggested by Leibler. Also, T_{ODT} depression and the change of D were compared with the theoretical predictions developed by Whitmore and Noolandi, and the experimental data fitted well within a reasonable range.

Acknowledgment. This work was supported by the Center for Advanced Functional Polymers and by POSTECH Research Fund. The assistance of the Pohang Accelerator Laboratory in performing SAXS measurements is gratefully acknowledged.

References and Notes

- (1) Leibler, L. *Macromolecules* **1980**, *13*, 1602.
- (2) Hashimoto, T.; Kimishima, K.; Hasegawa, H. *Macromolecules* **1991**, *24*, 5704.
- (3) de Gennes, P. G. *J. Phys. (Paris)* **1970**, *31*, 235.
- (4) Zin, W.-C.; Roe, R.-J. *Macromolecules* **1984**, *17*, 183.
- (5) Roe, R.-J.; Zin, W.-C. *Macromolecules* **1984**, *17*, 189.
- (6) Kang, C.-K.; Zin, W.-C. *Macromolecules* **1992**, *25*, 3039.
- (7) Matsen, M. W. *Macromolecules* **1995**, *28*, 5765.
- (8) Whitmore, M. D.; Noolandi, J. *Macromolecules* **1985**, *18*, 2846.
- (9) Winey, K. I.; Thomas, E. L.; Fetters, L. J. *Macromolecules* **1991**, *24*, 6182.
- (10) Nojima, S.; Roe, R.-J. *Macromolecules* **1987**, *20*, 1866.
- (11) Lee, H.-K.; Zin, W.-C. *Macromolecules* **2000**, *33*, 2894.
- (12) Shi, A.-C.; Noolandi, J.; Hoffmann, H. *Macromolecules* **1994**, *27*, 6661.
- (13) Kressler, J.; Karasz, F. *Makromol. Chem.* **1990**, *191*, 1623.
- (14) Cifra, P.; Karasz, F. E.; MacKnight, W. J. *Macromolecules* **1989**, *22*, 3649.
- (15) Kim, J. K. *Polymer* **1995**, *36*, 1243.
- (16) Jiang, M.; Huang, T.; Xie, J. *Macromol. Chem. Phys.* **1995**, *196*, 803.
- (17) Hong, K. M.; Noolandi, J. *Macromolecules* **1983**, *16*, 1083.
- (18) Fredrickson, G. H.; Leibler, L. *Macromolecules* **1989**, *22*, 1238.
- (19) de la Cruz, M. O. *J. Chem. Phys.* **1989**, *90*, 1995.
- (20) Lodge, T. P.; Hamersky, M. W.; Hanley, K. J.; Huang, C. I. *Macromolecules* **1997**, *30*, 6139.
- (21) Fredrickson, G. H.; Helfand, E. *J. Chem. Phys.* **1987**, *87*, 697.
- (22) Bates, F. S.; Rosedale, J. H.; Fredrickson, G. H. *J. Chem. Phys.* **1990**, *92*, 6255.
- (23) Barrat, J. L.; Fredrickson, G. H. *J. Chem. Phys.* **1991**, *95*, 1281.
- (24) Jeon, K.-J.; Roe, R.-J. *Macromolecules* **1994**, *27*, 2439.
- (25) Roe, R.-J.; Zin, W.-C. *Macromolecules* **1980**, *13*, 1221.
- (26) Stühn, B.; Mütter, R.; Albrecht, T. *Europhys. Lett.* **1992**, *18*, 427.
- (27) Floudas, G.; Hadjichristidis, N.; Iatrou, H.; Pakula, T.; Fischer, E. W. *Macromolecules* **1994**, *27*, 7735.
- (28) Almadal, K.; Rosedale, J. H.; Bates, F. S.; Wignall, G. D.; Fredrickson, G. H. *Phys. Rev. Lett.* **1990**, *65*, 1112.
- (29) Brazovskii, S. A. *Sov. Phys. JETP* **1975**, *41*, 85.
- (30) Bates, F. S. *Macromolecules* **1985**, *18*, 525.
- (31) Guenza, M.; Schweizer, K. S. *J. Chem. Phys.* **1997**, *106*, 7391.
- (32) Wolff, T.; Burger, C.; Ruland, W. *Macromolecules* **1993**, *26*, 1707.
- (33) Ogawa, T.; Sakamoto, N.; Hashimoto, T.; Han, C.-D.; Baek, D.-M. *Macromolecules* **1996**, *29*, 2113.
- (34) When S-B52/SBR50 is macroscopically phase-separated below the T_{ODT} , there is no difference in the refractive index between the lamellae microdomain and disordered SBR50 since S-B52 and SBR50 contain the same amount of styrene. We cannot distinguish between homogeneous and inhomogeneous phases by performing light scattering (LS) experiments. To measure the solubility limit of SBR50 on S-B52, the turbidity of the blend of S-B52/SBR60 was measured by a light scattering experiment. (The molecular weight of SBR60 is twice that of S-B52, and its styrene content is 60 wt %.) S-B52/SBR60 showed a macroscopically phase-separated state when the SBR60 content was larger than about 15 wt %.
- (35) Whitmore, M. D.; Noolandi, J. *J. Chem. Phys.* **1990**, *93*, 2946.

MA010593D